Measurement and Characterization of High Frequency Losses in Nonideal Litz Wires

Hans Rossmanith, Marc Doebroenti, Manfred Albach, and Dietmar Exner

***Abstract*—Commercially available litz wires are fabricated in several ways, depending on the number of strands and on the cost frame, either as twisted strands, as twisted bundles of twisted strands or as braided strands. The bundles have a finite pitch length, and the permutation of strands within this length is not perfect. This paper illustrates the effects of this nonideal construction on skin and proximity losses in the winding and indicates some applications where this may become important. Test setups have been developed to measure skin losses and proximity losses separately, thus offering the possibility of quantifying the quality of real litz wires by comparing the test results with the ideal behavior.**

***Index Terms*—Loss measurement, magnet wire, skin effect, windings.**

I. Introduction

LITZ wires have been used for windings in inductors and transformers of switch mode power supplies for a long time. Depending on the strand diameter, they offer reduced winding losses compared to solid wires of equal total cross section within a limited frequency range. This property has been described in several publications, e.g., [1]–[5]. Although in many applications a litz wire may be considered as ideal, i.e., with its total current equally distributed over the strands, for some cases a more realistic model should be used [6]. A similar situation is described in [7], where the losses of a spiral winding consisting of litz wires have been measured, and the test results do not match so well with the calculations, which are based on ideal litz wires.

In Section II, a test setup is presented that can be used to measure the skin losses (including the internal proximity losses inside the litz wire caused by the strands of the same wire) and the proximity losses due to external magnetic fields, caused by nearby wires and the core including the air gaps. This forms the basis for characterizing the deviations between real and ideal litz wires. Section III presents the theoretical background for calculating the losses in both situations, ideal and nonideal behavior. From the test results shown in Section IV, it becomes obvious that two scalar parameters are sufficient to characterize the nonideal properties of real litz wire for the two loss mechanisms skin losses (parameter λ_{skin}) and proximity losses (parameter λ_{prox}).

Manuscript received September 3, 2010; revised November 12, 2010 and February 4, 2011; accepted April 8, 2011. Date of current version November 18, 2011. This work was supported by the German Federal Ministry of Economics and Technology (BMWi) under Grant FKZ0327494A,B,C, upon decision of the German Bundestag. Recommended for publication by Associate Editor S. Y. (R.) Hui.

H. Rossmanith, M. Doebroenti, and M. Albach are with the Chair of Electromagnetic Fields, Erlangen University, Erlangen D-91058, Germany (e-mail: h.rossmanith@emf.eei.uni-erlangen.de; m.doebroenti@emf.eei.uni-erlangen.de; m.albach@emf.eei.uni-erlangen.de).

D. Exner is with Rudolf Pack GmbH & Co. KG, Gummersbach D-51645, Germany (e-mail: dietmar.exner@pack-feindraehte.de).

Color versions of one or more of the figures in this paper are available online at http://ieeexplore.ieee.org.

Digital Object Identifier 10.1109/TPEL.2011.2143729

II. Description of the Test Setup

A. Preparation of the Litz Wire Under Test

Litz wires are connected to the external circuit by solder joints. Since the strands are insulated individually, soldering must remove this insulation to provide a reliable electrical contact of all strands. At the same time, however, these solder joints are a path for eddy currents between the strands, which may increase the winding losses. In detail:

1) tests of litz wire properties will have to include these solder joints, if the wire length of the winding is comparable to or shorter than the pitch of the litz wire;
2) care must be taken to connect all strands, dc resistance measurement may be used to ensure this;
3) mechanical stress to the litz wire like bending, folding or squeezing will influence its electrical properties; so, the test setup should avoid mechanical stress to the litz wire under test as far as possible; and
4) exchanging the litz wire in the test setup should be easy and fast, because many samples have to be tested.

B. Winding Losses

If a time-dependent current

$$i(t) = i_0 + \sum_{n=1}^{\infty} \hat{i}_n \cos(n\omega t + \varphi_n) \tag{1}$$

is flowing through a solid round wire the losses P in this wire can be separated into rms losses and skin losses $P = P_{\mathrm{rms}} + P_{\mathrm{skin}}$ with

$$P_{\mathrm{rms}} = i_{\mathrm{rms}}^2 R_{\mathrm{dc}} = \left[i_0^2 + \frac{1}{2} \sum_{n=1}^{\infty} \hat{i}_n^2 \right] R_{\mathrm{dc}} \tag{2}$$

and

$$P_{\mathrm{skin}} = \left[\left(\frac{1}{2} \right) \sum_{n=1}^{\infty} \hat{i}_n^2 \cdot (F_{sn} - 1) \right] R_{\mathrm{dc}} \text{ with}$$

$$F_{sn} = \frac{1}{2} \operatorname{Re} \left\{ \alpha_n a \frac{I_0(\alpha_n a)}{I_1(\alpha_n a)} \right\}, \quad \alpha_n = \frac{1+j}{\delta_n},$$

$$\delta_n = \sqrt{\frac{2}{n\omega\sigma_{\mathrm{Cu}}\mu}}. \tag{3}$$

F_{sn} is the skin factor at the frequency of the nth harmonic, a is the radius of the wire, δ_n is the skin depth, and I_0 and I_1 are the modified Bessel functions of the first kind of orders 0 and 1, respectively, σ_{Cu} is the conductivity of copper.

If the wire is located in an external magnetic field an additional loss mechanism occurs. With a field orientation perpendicular to the axis of the wire and a homogeneous field distribution these so-called proximity losses are given by the relation

$$P_{\mathrm{prox}} = \frac{l}{\sigma_{\mathrm{Cu}}} \hat{H}_{\mathrm{ext}}^2 \cdot D_s \quad \text{with} \quad D_s = 2\pi \mathrm{Re}\left\{ \frac{\alpha a I_1(\alpha a)}{I_0(\alpha a)} \right\} \tag{4}$$

where $\hat{H}_{\mathrm{ext}}$ is the amplitude of the external field, l is the wire length, and D_s is the proximity factor for the solid wire. For the more general situation with an inhomogeneously distributed external field, e.g., inside the winding area caused by air gaps, the procedure of how to solve this problem is given in [8].

In case of litz wires the situation is more complicated, because each strand is located in the field caused by the other strands in the same bundle. A homogeneous external field will generate eddy currents inside the strands. Significant inhomogeneous fields produced by these eddy currents will only occur at high frequencies. Even then, these stray fields have line dipole characteristics and compensate each other inside a litz wire with circular cross section and a sufficiently large number of strands. Preliminary simulations (finite elements) of a litz wire type 30 mm $\times$ 0.2 mm with and without these stray fields resulted in closely matching total proximity losses, with deviations less than 2% from 1 kHz to 30 MHz. So, the simple formula (4) seems to be adequate for the proximity losses not only of single strands but also of complete litz wire bundles in the investigated frequency range. At even higher frequencies corrections may be made using the method in [9].

Even if no external field from outside the litz wire, e.g., caused by nearby wires or the core with the air gaps, is taken into account, we will get "internal proximity losses." In the literature, the total losses are sometimes separated into rms losses, strand-level skin losses, bundle-level skin losses, internal strand-level proximity losses, external strand-level proximity losses, and bundle-level proximity losses.

From a practical point of view, these six categories should be lumped into only three groups.

1) "RMS losses" (as defined earlier): They can be influenced by the length and the cross-sectional area of the wire.
2) "Skin losses of the litz wire": This is the combination of all skin losses in the whole bundle and the proximity losses in all strands, but only those caused by the field from the other strands in the same litz wire. There are two major reasons for this combination of losses. If we measure the frequency-dependent resistance of a certain length of the litz wire, e.g., with an impedance analyzer, the increasing resistance with frequency is caused by exactly these losses. The second reason is that this resistance can be influenced by the manufacturing process of the litz wire, because it depends on the number of strands, on the diameter of the strands, on the outer shape of the bundle, on the pitch length, and also on the number of strands of subbundles.
3) "Proximity losses": These are the proximity losses in the whole bundle, but only those caused by external fields, e.g., from the other wires, from the core, and from the air gaps. These losses can be influenced by the design of the inductive component, e.g., by the number of layers, by the number of turns in a layer, by the position of the turns in the winding area, by the position of the air gaps, and so on.

By separating the total losses into these three groups, we can do the same measurement for solid wires and litz wires and we are able to directly compare solid wires and different types of litz wires.

For circular litz wires with strands of circular cross section, these types of winding losses can be shown to be orthogonal [10], so they may be calculated separately and added up. Also, solid wires with circular cross section may be treated in this way. To measure these types of losses separately, however, turns out to be a challenge. In the following chapters, we will present suitable test setups.

C. RMS and Skin Losses

The value of R_{dc} can easily be measured using a microohmmeter with Kelvin clamps, but it can also be calculated in a simple way. This may become useful when verifying the quality of solder joints between litz wires. Of course, the length of the strands has to be used in this calculation, which is a few percent larger than the length of the bundle. Nevertheless, some uncertainty remains, mainly because of the tolerance of the strand diameter.

Skin losses appear at higher frequencies as an additive term to rms losses. A measurement of small skin losses compared to rms losses will tend to be not very accurate, since subtraction is involved. But in this case, they will have no great impact on the total losses.

For the measurement setup, several problems had to be overcome.

1) Proximity losses due to the magnetic field of nearby wires have to be avoided.
2) Proximity losses in nearby metallic structures, as well as magnetic losses in nearby iron structures, including the test equipment, have to be avoided.
3) The inductance of the test setup must be kept low, since otherwise, the phase angle will be too small and loss measurements will become inaccurate [11].
4) The litz wire under test must not experience mechanical stress during the tests to ensure reproducible results.

Fig. 1 shows the final test setup used to measure the skin losses of litz wires.

The litz wire to be tested is inserted into a circular groove through a brass bar of length 1 m to form the inner conductor of a coaxial waveguide. Setups of different groove sizes have been manufactured to match the various litz wire diameters. In the examples here, a groove diameter of 6 mm was selected. Spacers of appropriate inner diameter are used to center the litz wire. At the far end, the litz wire is connected to the bar. At the near end, the impedance Z is measured via an impedance

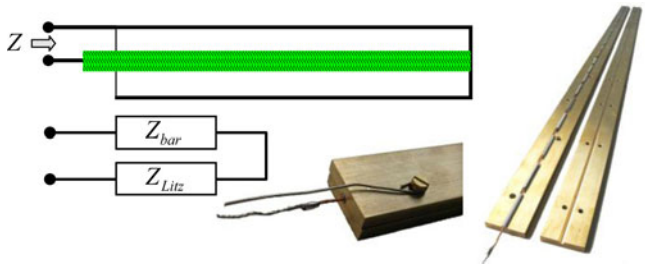

Fig. 1. Test setup to measure skin losses in litz wires via an impedance analyzer.

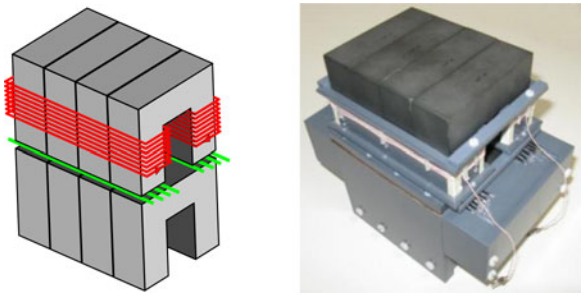

Fig. 2. Test setup for the proximity effect measurements.

analyzer. The real part of this impedance characterizes the total losses of litz wire and brass bar. Because the dc resistance of the litz wire is known as well as the frequency-dependent loss resistance of the brass bar, e.g., from measurements with solid wires, the skin loss resistance of the litz wire can be extracted from the measurement result Z

$$R_{\mathrm{skin}} = \mathrm{Re}\{Z - Z_{\mathrm{bar}}\} - R_{\mathrm{dc}}. \tag{5}$$

As will be illustrated later, the total test setup forms a transmission line, so (5) will hold only for frequencies where the wavelength is large compared to the length of the waveguide. Higher frequencies will be treated with a modified approach. This test setup does not generate any (external) proximity losses in the litz wire or outside the bar.

D. Proximity Losses

Whereas the combination of rms and skin losses, discussed so far, describes the frequency-dependent behavior of the wire and, thus, characterizes the wire type, the proximity losses always occur, if the wire is used to realize a winding with several turns, either with additional core or not.

With the test setup shown in Fig. 2, only the so-called external proximity losses will be evaluated (the third loss mechanism described earlier). As we tried to avoid calorimetric test equipment, the proximity losses in the device under test (DUT) had to be detected by an increase of loss in an excitation coil. Reliable test results, however, can only be obtained by taking the following rules into consideration.

1) Keep the losses in the excitation coil low and in the DUT high.
2) Keep the magnetic stray field low, so that no other structures in the neighborhood generate losses.
3) Use a test setup where the magnetic field in the DUT can be determined easily.
4) Avoid stray capacitances in the test setup, especially those connected with the DUT.
5) Avoid magnetic field distortion by the DUT, or include it in the theory.
6) Use air coils, or if necessary, use low-loss magnetic material.

The test setup for proximity effect measurements consists of a magnetic circuit with four parallel UI-combinations of U93/76/30 cores with air gaps, similar to [6]. The litz wire samples to be tested were placed in the air gaps and, thus, exposed to a high magnetic field intensity. The material of the U-cores is Ferroxcube 3F4, which has low core losses up to several megahertz. The width of the two air gaps can be adapted to fit different litz wire diameters.

An excitation coil of 16 turns was connected to an impedance analyzer. Its dc resistance is 0.5 Ω. Above 300 kHz, for the air gap size 3 mm, core losses become dominant. In the test setup of Fig. 2, the proximity losses in the litz wire samples (DUT) were calculated by comparing the impedances Z_0 of a reference measurement without DUT to the actual measurement Z with DUT.

First measurements used litz wires of a length greater than 1 m, which were bent several times to fit inside the air gaps. It became clear very soon that these samples, with strands insulated at the ends, would only behave like ideal litz wires. Nonideal effects of connected strands could only be observed when using short samples (compared to the pitch), with solder joints at each end.

However, the litz wire samples to be tested had to be long enough so that the solder joints at both ends could be placed sufficiently far away from the air gaps and the fringing field would not produce extra proximity losses in them. We chose sections of 15.5 cm length, of which six were placed inside each of the two air gaps.

The real parts of the measured impedances, R_0 (without DUT) and R (with DUT) determine the power loss in the test setup of both configurations. As a first approximation, their difference is the proximity loss in the DUT

$$P_{\mathrm{DUT}} = \frac{1}{2}(R - R_0)\,\hat{i}^2. \tag{6}$$

The magnetic field amplitude at each sample of the DUT is calculated by analysis of the magnetic circuit. Its mean square over the DUT

$$\overline{\hat{H}^2_{\mathrm{ext}}(\mathrm{DUT})} = \overline{h^2_{\mathrm{DUT}}}\,\hat{i}^2 \tag{7}$$

is proportional to the proximity losses in the DUT. With the dc-conductivity σ_{Cu} and the total length l of the DUT inside the field as normalizing factors, the proximity factor of the DUT is defined by

$$D_s = \frac{\sigma_{\mathrm{Cu}}}{l}\frac{P_{\mathrm{DUT}}}{\overline{\hat{H}^2_{\mathrm{ext}}(\mathrm{DUT})}} = \frac{\sigma_{\mathrm{Cu}}}{2l}\frac{R - R_0}{\overline{h^2_{\mathrm{DUT}}}}. \tag{8}$$

It can be used to characterize the proximity losses of the litz wire under test.

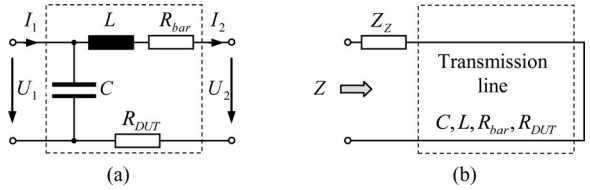

Fig. 3. (a) Equivalent circuit of subsection. (b) Equivalent circuit of test set-up. Z_Z: contact impedance, $R_{\rm bar}$: brass bar resistance, $R_{\rm DUT}$: litz wire resistance, C: transmission line capacitance, L: transmission line inductance.

As the proximity losses in solid wires can easily be calculated, the validity of the described test procedure can be checked by applying this measurement to solid wires and comparing both calculated and measured results.

III. Theoretical Background

Because winding losses are linear, the Fourier expansion of arbitrary periodic current wave shapes can be used to sum up the losses of all harmonic components. For this reason, it is sufficient to restrict the investigations to sinusoidal currents with different frequencies.

A. Skin Losses

Skin and internal proximity losses in ideal round litz wires have been calculated, e.g., in [1]. These calculations assume an equal current distribution over all strands, so that each one of the N strands carries a current with the same amplitude $\hat{i}/N$ and the same phase. This type will be referred to as "ideal litz wire." In practice, this requires interchanging the strands of the litz wire with a pitch which is short compared to the total wire length. For comparison, also, skin losses of a bundle of parallel strands have been calculated. In the bundle, the strands do not exchange their positions, and the current in the strands will vary according to the strand position in the bundle. Current distribution and losses of parallel strands are equivalent to those of a solid round wire with the same diameter as the bundle, if the solid wire conductivity is reduced appropriately. The conductivity of the solid wire was adjusted such that the dc resistance of the solid wire matches that of the bundle of parallel strands [see (17)].

To calculate the behavior of ideal litz wires and parallel strands in the test setup shown in Fig. 1, the length of the setup is subdivided into M (e.g., $M = 100$) separate sections. Each subsection can be described by the equivalent circuit in Fig. 3(a).

With the currents i_1, i_2 and voltages u_1, u_2 defined in Fig. 3(a), the chain matrix of the circuit is given by

$$\begin{pmatrix} u_1 \\ i_1 \end{pmatrix} = \Delta\mathbf{A} \begin{pmatrix} u_2 \\ i_2 \end{pmatrix};$$

$$\Delta\mathbf{A} = \begin{pmatrix} 1 & R_{\rm DUT} + R_{\rm bar} + Z_L \\ Y_C & 1 + Y_C(R_{\rm DUT} + R_{\rm bar} + Z_L) \end{pmatrix}. \quad (9)$$

Here, $Z_L = j\omega L$ describes the impedance of the inductance L, and $Y_C = j\omega C$ the admittance of the capacitance C in this subsection. The total test setup is shown in Fig. 3(b). Here, all M subsections are connected in chain to form a transmission line. Its far end is short-circuited; its near end is connected to the impedance analyzer ports. The impedance Z_Z comprises a contact resistance of the terminal connections to the impedance analyzer as well as an inductance of the connecting leads to these terminals.

The chain matrix of the transmission line is

$$\mathbf{A} = (\Delta\mathbf{A})^M = \begin{pmatrix} a_{11} & a_{12} \\ a_{21} & a_{22} \end{pmatrix}. \quad (10)$$

From this, the impedance of the test setup is calculated as

$$Z = Z_Z + \frac{a_{12}}{a_{22}}. \quad (11)$$

This impedance Z, evaluated for ideal litz wires and parallel strands, will be the basis for comparing the measurement results for the skin effect in real litz wires.

The different behavior of real litz wires with respect to ideal litz wires is due to the fact, that the strands are not perfectly interchanged, even in the case of samples that are long compared to the pitch length. For this reason, it is expected, that real litz wires show a behavior somewhere between ideal litz wires and parallel strands. More than 70 types of litz wires, with varying number of strands (6 . . . 2550), strand diameters (0.04 . . . 0.5 mm), pitch lengths, subbundle configurations, and cross sections were analyzed. All samples had a frequency-dependent resistance R_λ that could be described by a linear combination of that of an ideal litz wire $R_{\rm id}$ and of parallel strands $R_{\rm par}$, typically with maximal deviations over the total frequency range (10 kHz . . . 30 MHz) much less than 10%. We encountered no example where a single scalar parameter $\lambda_{\rm skin}$ was not sufficient to describe this behavior over the full frequency range, by

$$R_\lambda = \lambda_{\rm skin}\, R_{\rm id} + (1 - \lambda_{\rm skin}) R_{\rm par}. \quad (12)$$

This parameter $\lambda_{\rm skin}$ takes the role of a quality parameter: $\lambda_{\rm skin} = 1$ means perfect litz wire, where the total current is distributed equally over the strands and $\lambda_{\rm skin} = 0$ means parallel strands with skin losses like an equivalent solid wire. Both extreme cases can be calculated analytically with sufficient accuracy.

Equation (13) gives the analytical formula used to describe the frequency-dependent resistance of an ideal litz wire due to skin effect, similar to [1]

$$R_{\rm id} = R_{\rm dc} \frac{1}{2} {\rm Re}\left\{ x_S \left[\frac{I_0(x_S)}{I_1(x_S)} + N(N-1) \frac{d_S^2}{d_L^2} \frac{I_1(x_S)}{I_0(x_S)} \right] \right\}. \quad (13)$$

The model of an equivalent solid wire is used for the bundle of parallel strands

$$R_{\rm par} = R_{\rm dc} \frac{1}{2} {\rm Re}\left\{ x_L \frac{I_0(x_L)}{I_1(x_L)} \right\}. \quad (14)$$

The complex arguments x_S and x_L are the normalized skin parameters of a single strand and of the equivalent solid wire,

respectively

$$x_S = (1+j)\sqrt{\pi f \mu_0 \sigma_{\mathrm{Cu}}}\frac{d_S}{2}, \quad x_L = (1+j)\sqrt{\pi f \mu_0 \sigma_L}\frac{d_L}{2} \tag{15}$$

where d_S is the diameter of a single strand of the litz wire, N is the number of strands, d_L is the diameter of the total litz wire (the same as that of the equivalent solid wire), given by

$$d_L = d'_S\sqrt{\frac{2}{\pi}\sqrt{3}N} \tag{16}$$

where d'_S is the distance between two strands in the litz wire, which is somewhat greater than the strand diameter, due to the additional insulation of the strands. The conductivity σ_L is chosen such that dc-losses of equivalent solid wire and parallel strands match

$$\sigma_L = \sigma_{\mathrm{Cu}}\frac{d_S^2 N}{d_L^2}. \tag{17}$$

The dc resistance R_{dc} of the litz wire of length l (which is here considered as equal to that of the parallel strands) is

$$R_{\mathrm{dc}} = \frac{4l}{\sigma_{\mathrm{Cu}}\pi d_S^2 N}. \tag{18}$$

Actually, also the transmission line impedance Z in Fig. 3(b) [calculated by (11)] with a real litz wire as center conductor can be expressed as a linear combination according to (12), with the same parameter λ_{skin}.

B. Proximity Losses

Proximity losses of round litz wires in a homogeneously distributed magnetic field have been calculated, e.g., in [2] or [12]. For round litz wires with N strands, the proximity losses are very close to N times the proximity loss of one single strand, within the total frequency range. However, only ideal litz wires are considered, where the current in each strand cancels out to zero.

The proximity losses in an ideal litz wire due to a homogeneous external magnetic field can be calculated analytically. A good approximation according to Section II-B will be

$$P_{\mathrm{prox,id}} = \frac{l}{\sigma_{\mathrm{Cu}}}\hat{H}_{\mathrm{ext}}^2 \cdot N D_{\mathrm{id}} \quad \text{with}$$
$$D_{\mathrm{id}} = 2\pi \mathrm{Re}\left\{\frac{x_S\, I_1(x_S)}{I_0(x_S)}\right\}. \tag{19}$$

As before, x_S is the normalized skin parameter of a single strand according to (15). If the strands in the litz wire are connected to each other, e.g., by solder joints, the strand current in each strand will not cancel out to zero any more. The extreme case would be a bundle of parallel strands, which are electrically parallel connected. Its current distribution over the bundle cross-section matches that of an equivalent single solid wire of equal diameter. The conductivity of the equivalent solid wire is adapted to account for the copper filling factor according to (17). The proximity losses for the bundle with parallel strands are then

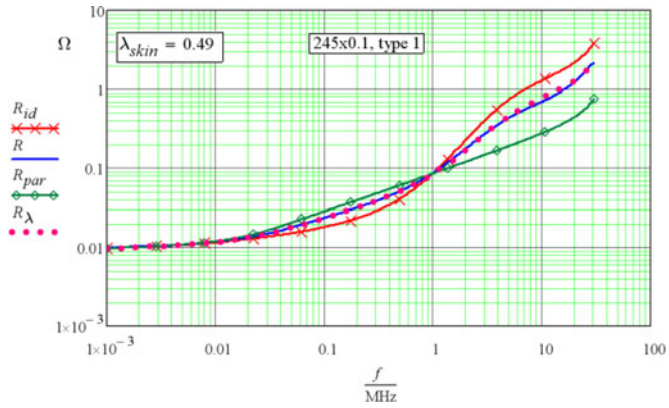

Fig. 4. Frequency-dependent resistance of the transmission line in Fig. 3(b) for ideal litz wire R_{id}, parallel strands R_{par}, a linear combination of both [R_{λ}, from (12)] and measurement result R for sample 245 × 0.1, type 1.

given by

$$P_{\mathrm{prox,par}} = \frac{l}{\sigma_L}\hat{H}_{\mathrm{ext}}^2 \cdot N D_{\mathrm{par}} \quad \text{with}$$
$$D_{\mathrm{par}} = \frac{2\pi}{N}\mathrm{Re}\left\{\frac{x_L\, I_1(x_L)}{I_0(x_L)}\right\} \tag{20}$$

where x_L is the normalized skin parameter of the equivalent solid wire according to (15).

Sections of litz wires without solder joints show ideal behavior with respect to proximity effect, i.e., the total current of each strand cancels to zero. However, in real applications, litz wire windings have to be soldered to contact pins, so the strands are not isolated from each other. As a consequence, like skin losses, proximity losses in litz wires may not always behave in this ideal way. Solder joints at short distance will have an influence, which should be tested. It is expected, that a distance of solder joints shorter than the pitch of the litz wire will push the proximity losses near to those of parallel stranded wires.

IV. Measurement Results

Two types of litz wires, having all the same number of strands with the same diameter, are investigated (245 mm × 0.1 mm). Only the inner structure of these two types is different: type 1 is made of seven bundles, each of 35 strands, type 2 is made of four bundles, each of 61 or 62 strands. The pitch length at bundle level of both types is 3.7 cm, at strand level 2.9 cm. Both types are wrapped with a double layer of polyamide yarn. Skin and proximity effect measurements show quite different behavior.

A. Skin Losses

Real litz wires have skin losses that lie in between those of ideal litz wires (calculated under assumption of an equally distributed current among the strands) and those of parallel strands. This model is valid over the total frequency range, with some caution at very high frequencies.

Figs. 4 and 5 show the frequency-dependent resistance of the test setup with 1.07 m length of litz wire, which comprises ohmic, skin, and internal proximity losses. Both figures display

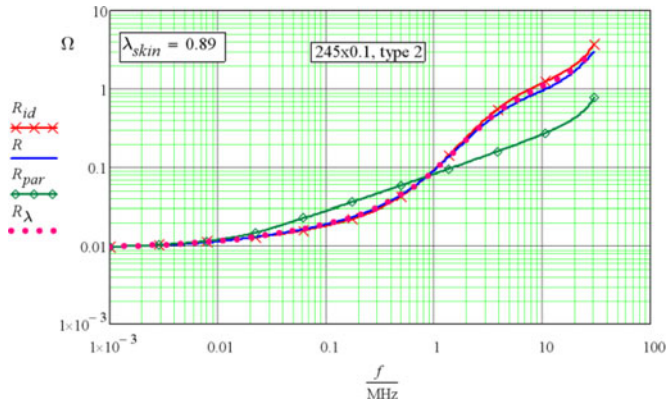

Fig. 5. Frequency-dependent resistance of the transmission line in Fig. 3(b) for ideal litz wire R_{id}, parallel strands R_{par}, a linear combination of both [R_{λ}, from (12)] and measurement result R for sample 245 × 0.1, type 2.

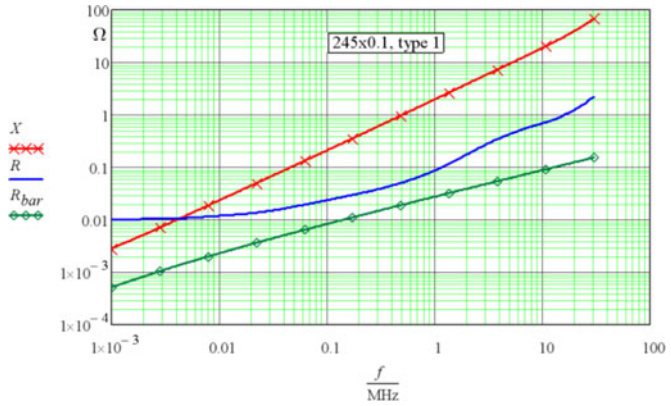

Fig. 6. Reactance X, total resistance R, and contribution R_{bar} of the brass bar to the total resistance.

quite large differences between these two litz wire types. The theoretical losses (ideal litz wire R_{id} and equivalent solid wire or parallel strands R_{par}, respectively) in the two figures are the same, measurement results and adapted theoretical curves for real litz wire are not. All theoretical curves have been calculated as to be comparable to the skin effect measurement by means of the brass bar in Fig. 1.

To confirm the validity of the results, Fig. 6 compares the reactance X, the total resistance R, and the calculated contribution R_{bar} of the brass bar. R_{bar} is small compared to R, and X compared to R is in a range, where the test results obtained from the impedance analyzer are sufficiently accurate.

An off-center position of the litz wire under test can be shown to increase the resistance of the brass bar by a factor

$$f_{\mathrm{bar}} = \frac{1+4c^2}{1-4c^2} \tag{21}$$

where c is the off-center distance of the litz wire divided by the groove diameter. Equation (21) holds exactly for skin depth equal to zero, but is also a good approximation for the frequency range under consideration. An evaluation of (21) shows that the influence of c can be neglected as long as it is less than 10%.

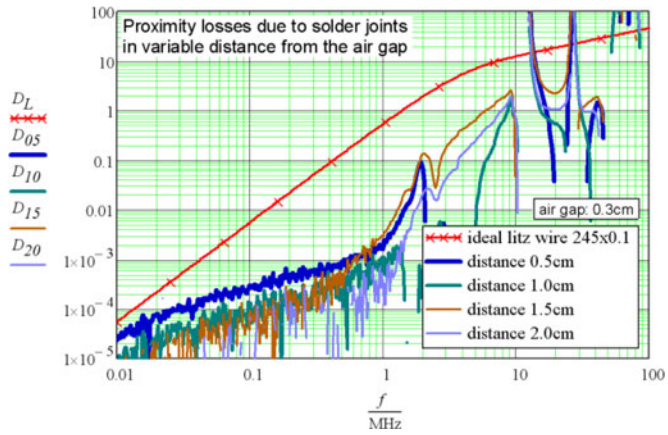

Fig. 7. Normalized proximity losses of litz wire and solder joints.

B. Proximity Losses

Measurements with open-ended litz wires are in very good agreement with the ideal theoretical results (see Fig. 8). Deviations from the ideal behavior at very low frequencies can be explained by the finite measurement accuracy due to dominant dc losses in the excitation coil, which becomes noticeable for very small proximity losses. A measurement setup as in [6] with separate excitation and measurement coils could eliminate these errors.

To measure deviations in the proximity effect of real litz wires from ideal behavior is not as easy. It was necessary to use quite small sections of litz wire with solder joints at both ends and put the sections under the influence of an external magnetic field. However, the solder joints themselves have the proximity losses at lower frequencies that dominate the measurement. Of course, the proximity losses of solder joints provide no further insight, so this effect had to be eliminated.

In the test setup of Fig. 2, the litz wire samples to be tested had to be so long that the solder joints at both ends could be placed far enough from the air gap, so the fringing field would not produce extra proximity losses in them. We chose sections of 15.5 cm length, of which up to six were placed inside each of the two air gaps. With a core length of 12 cm, the distance of the solder joints from the air gap on each side was 1.7 cm. So, for the air gap width of 3 mm, the air gap stray field did not generate significant losses in the solder joints. The greater total length of the sections compared with the length inside the air gap field was taken into account mathematically. Fig. 7 shows the influence of solder joints in the vicinity of the air gap. For this measurement, the soldered ends of the litz wire samples under test were placed at variable distance from the air gaps, with no wires in the air gaps themselves. Even at the shortest distance 0.5 cm, losses in the solder joints were much lower than the proximity losses in the litz wire samples.

The measurement provides a value P_{prox} for the proximity losses in the litz wire under test. In all tested litz wire samples, this value lies between the calculated values $P_{\mathrm{prox,id}}$ (19) and $P_{\mathrm{prox,par}}$ (20). In fact, a linear combination as in (12) can be

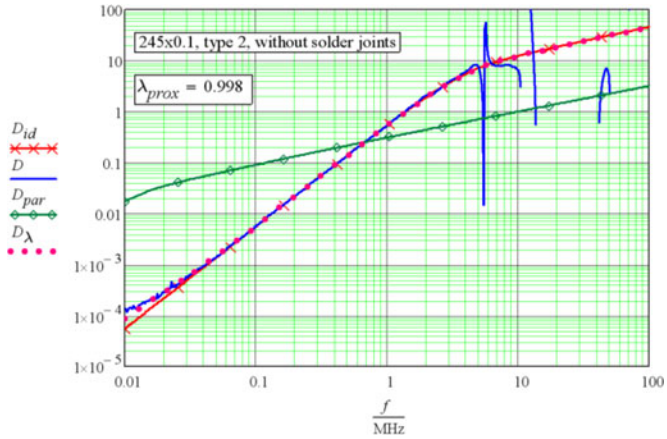

Fig. 8. Proximity factor for 15.5-cm-long sections of litz wire 245 × 0.1, type 2 without solder joints.

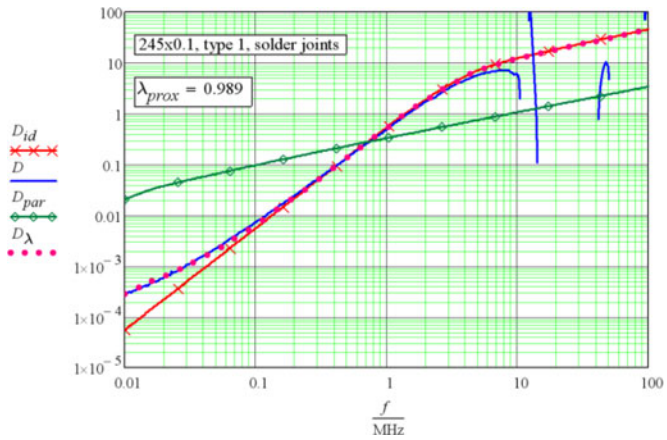

Fig. 9. Proximity factor for 15.5-cm-long sections of litz wire 245 × 0.1, type 1 with solder joints at the ends.

used for an approximation of the test results

$$P_{\mathrm{prox},\lambda} = \lambda_{\mathrm{prox}}\, P_{\mathrm{prox,id}} + (1-\lambda_{\mathrm{prox}})\, P_{\mathrm{prox,par}}. \qquad (22)$$

Again, this scalar parameter λ_{prox} can be regarded as a quality factor for the litz wire under test with respect to the proximity losses. It is to be noted, that the parameter λ_{prox}—contrary to λ_{skin}—varies with the length of the litz wire samples, (see Fig. 11). In order to be independent of the applied magnetic field, proximity factors are calculated from the proximity losses

$$D = \frac{\sigma_{\mathrm{Cu}}}{l\hat{H}^2_{\mathrm{ext}}N}\, P_{\mathrm{prox}}, \quad D_\lambda = \frac{\sigma_{\mathrm{Cu}}}{l\,\hat{H}^2_{\mathrm{ext}}N}\, P_{\mathrm{prox},\lambda}. \qquad (23)$$

To verify the validity of (22), Figs. 8–10 compare the proximity factor D calculated from measurement data with the proximity factor D_λ calculated from the approximation (22).

Compared to the differences found in skin effect measurements, the proximity effect measurements do not differ as much for the two different types of litz wire (see Figs. 9 and 10). Thirteen centimeters of each litz wire section have been exposed to the magnetic field, which is larger than the pitch lengths 3.7 cm (bundles) and 2.9 cm (strands), so the deviation from ideal behavior is small and mainly visible in the lower frequency range.

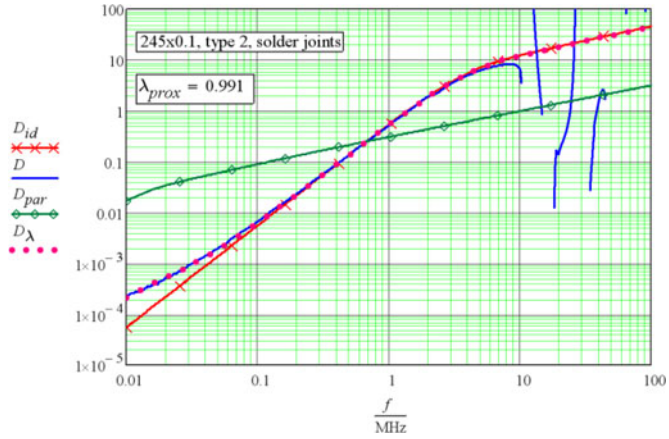

Fig. 10. Proximity factor for 15.5-cm-long sections of litz wire 245 × 0.1, type 2 with solder joints at the ends.

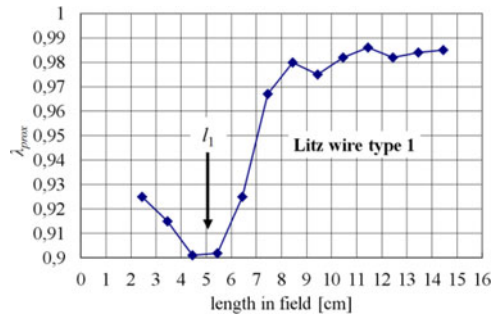

Fig. 11. Quality parameter (proximity effect) of litz wire 245 × 0.1, type 1 with solder joints at the ends for varying lengths exposed to the magnetic field.

At high frequencies, the proximity losses of real litz wires are close to the losses of ideal litz wires. Above 10 MHz, the inherent core losses of the test setup exceed the losses in the wires and reliable test results cannot be expected.

C. Evaluation of Results

In real litz wires, the current is not equally distributed between the strands, due to nonperfect interchange of the strands. There are several construction parameters that have an influence. Not only the pitch length plays an important role, but also the substructure of the bundle.

In proximity effect measurements, the quality parameter λ_{prox} correlates to the length of the litz wire which is exposed to the magnetic field. Fig. 11 shows a sample of litz wire type 1 with total length 15.5 cm and solder joints at the ends, which has been exposed to the magnetic field at varying lengths. A typical valley occurs near $l_1 = 5$ cm, which corresponds to 1.5 pitch lengths at bundle level and 2 pitch lengths at strand level. At this length, the magnetic flux through a loop formed of two strands will have a maximum, leading to a peak in the proximity losses at bundle level. At the length 9.5 cm, a smaller valley is visible. In cases of greater lengths subjected to the field, these effects tend to cancel out, so that no more valleys are visible.

In skin effect measurements, the pitch length is correlated to the quality parameter λ_{skin}. This parameter is independent of

TABLE I
INFLUENCE OF LITZ WIRE PITCH

type	1a	1	1b	2
bundle pitch	2.0cm	3.7cm	4.5cm	3.7cm
strand pitch	2.9cm	2.9cm	2.9cm	2.9cm
l_1	2.5cm	5.0cm	6.5cm	5.0cm
λ_{skin}	0.58	0.49	0.43	0.89
λ_{prox}	0.991	0.989	0.983	0.991

the sample length when the test samples are long compared to the pitch length.

Table I shows the measurement results of four litz wire types: types 1a, 1, and 1b are built from seven bundles of 35 strands each, but with different pitch lengths. Type 2 (four bundles of 61 and 62 strands) is included, too. For otherwise equal inner structure, both quality parameters decrease with increasing bundle pitch length of the litz wire. A modified bundle substructure like that of type 2, however, has by far the greatest influence.

V. CONCLUSION

A new test setup has been presented, which offers the possibility for measuring the frequency-dependent resistance of a single litz wire without the influence of nearby currents or metallic/permeable objects. The obtained test results indicate that a single scalar value can be used to characterize the quality of a real litz wire over the full frequency range. Measured and theoretical results for the frequency-dependent resistance of the nonideal litz wire can be brought into very good agreement by adjusting this parameter. Skin effect is dominant in energy transmission over wires at higher frequencies. If litz wires are chosen to limit the skin losses, their nonperfect properties must be taken into account.

A second test setup has been used to evaluate the proximity effect of litz wires independent of the skin losses and without the influence of metallic or soft magnetic objects in the vicinity. Measurements of the proximity effect in round litz wires show quite good agreement with the theoretical results for the ideal litz wires. Nonideal behavior has been observed if solder joints in short distances are present. One additional scalar parameter λ_{prox} is sufficient to describe the nonideal behavior of a certain length of litz wire in case of the proximity effect.

This paper shows that the nonideal behavior of any given litz wire at skin effect may be described by only one scalar parameter. This parameter in combination with the well-known analytical formulas for skin losses in ideal litz wires and equivalent solid wires offers the possibility to describe the actual skin losses in real litz wires, where strands are not perfectly interchanged. With respect to the proximity effect, this paper characterizes a real litz wire by a second scalar parameter. This parameter λ_{prox} is influenced by the length of the litz wire which is exposed to the external field. Lengths that are smaller or comparable to the pitch length will lead to reduced values λ_{prox}, thus increasing the proximity losses especially at lower frequencies.

For certain subbundle configurations, a single parameter λ_{prox} may not be sufficient to describe the proximity losses within the whole frequency range. A better description would comprise parameters for subbundles as well, a subject for further research.

REFERENCES

[1] A. W. Lotfi and F. C. Lee, "A high frequency model for litz wire for switch-mode magnetics," in *Proc. IEEE Ind. Appl. Conf. 1993, Conf. Rec. IAS Annu. Meeting*, 2011, vol. 2, pp. 1169–1175.
[2] M. Bartoli, N. Noferi, A. Reatti, and M. K. Kazimierczuk, "Modeling litz-wire winding losses in high-frequency power inductors," in *Proc. IEEE Power Electron. Spec. Conf.*, 1996, vol. 2, pp. 1690–1696.
[3] C. R. Sullivan, "Optimal choice for number of strands in a litz-wire transformer winding," *IEEE Trans. Power Electron.*, vol. 14, no. 2, pp. 283–291, Mar. 1999.
[4] J. Schutz, J. Roudet, and A. Schellmanns, "Modeling litz wire windings," in *Proc. IEEE Ind. Appl. Conf. 1997, Conf. Rec. 32nd IAS Annu. Meeting*, vol. 2, pp. 1190–1195.
[5] S. Wang, M. A. Rooij, W. G. Odendaal, J. D. van Wyk, and D. Boroyevich, "Reduction of high-frequency conduction losses using a planar litz structure," *IEEE Trans. Power Electron.*, vol. 20, no. 2, pp. 261–267, Mar. 2005.
[6] X. Tang and C. R. Sullivan, "Stranded wire with uninsulated strands as a low-cost alternative to litz wire," in *Proc. IEEE Power Electron. Spec. Conf.*, 2003, vol. 1, pp. 289–295.
[7] J. Acero, R. Alonso, J. M. Burdio, L. A. Barragan, and D. Puyal, "Frequency-dependent resistance in litz-wire planar windings for domestic induction heating appliances," *IEEE Trans. Power Electron.*, vol. 21, no. 4, pp. 856–866, Jul. 2006.
[8] M. Albach, "Two-dimensional calculation of winding losses in transformers," in *Proc. IEEE Power Electron. Spec. Conf.*, 2000, vol. 3, pp. 1639–1644.
[9] X. Nan and C. R. Sullivan, "An equivalent complex permeability model for litz-wire windings," *IEEE Trans. Ind. Appl.*, vol. 45, no. 2, pp. 854–860, Mar./Apr. 2009.
[10] J. A. Ferreira, "Analytical computation of ac resistance of round and rectangular litz wire windings," *IEE Proc. B Electr. Power Appl. U.K.*, vol. 139, no. 1, pp. 21–25, Jan. 1992.
[11] S. Prabhakaran and C. R. Sullivan, "Impedance-analyzer measurements of high-frequency power passives: Techniques for high power and low impedance," in *Proc. IEEE Ind. Appl. Conf. 2002, Conf. Rec. 37th IAS Annu. Meeting*, vol. 2, pp. 1360–1367.
[12] F. Tourkhani and P. Viarouge, "Accurate analytical model of winding losses in round Litz-wire windings," *IEEE Trans. Magn.*, vol. 37, no. 1, pp. 538–543, Jan. 2001.
[13] X. Nan and C. R. Sullivan, "An improved calculation of proximity-effect loss in high-frequency windings of round conductors," in *Proc. IEEE Power Electron. Spec. Conf.*, 2003, vol. 2, pp. 853–860.

Hans Rossmanith received the Dr.-Ing. degree from Erlangen University, Germany, in 1990.

Since 1993, he has been a Scientific Assistant in the Department of Electrical Engineering, Electronics and Information Technology, Friedrich-Alexander-University, Erlangen-Nuremberg, Bavaria, Germany. In 1999, he joined the Chair for Electromagnetic Fields. His research interests include electromagnetic field theory, electromagnetic compatibility, and numerical field calculation.

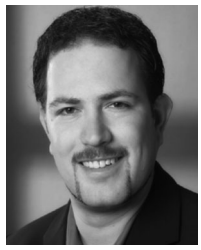

Marc Doebroenti He studied electrical engineering at Friedrich-Alexander-University, Erlangen-Nuremberg, Bava-ria, Germany, where he received the Dipl.-Ing. degree in 2009.

Since 2009, he has been a Research Assistant with the main focus on the project "Characterization and optimization of litz wire windings in chokes and transformers for higher energy efficiency."

Manfred Albach received the Dr.-Ing. degree from Technical University Berlin, Germany, in 1982.

Since 1999, he has been holding the Chair for Electromagnetic Fields of Friedrich-Alexander-University, Erlangen-Nuremberg, Bavaria, Germany. His research interests include a.o. the Maxwell field theory as well as power electronics with the focus on electromagnetic compatibility and inductive components.

Dietmar Exner received the Dipl.-Ing. degree in mechanical engineering from Koeln University of Applied Science, Gummersbach, Germany, in 1999.

He has been an Assistant to the Management at Rudolf Pack GmbH & Co. KG, Gummersbach, Germany, since 1999. He is responsible for customer support and the implementation of the customer requests within the company.